UDC 544.463:[546.55/.59+546.72:546.261]

# Mechanosynthesis of Cu–$Fe_3C$ Nanocomposites Using Liquid Hydrocarbon

M. A. EREMINA, S. F. LOMAEVA, E. P. ELSUKOV, A. L. ULYANOV and A. A. CHULKINA

*Physical-Technical Institute, Ural Branch of the Russian Academy of Sciences, Ul. Kirova 132, Izhevsk 426000 (Russia)*

*E-mail: mrere@mail.ru*

## Abstract

Features of the formation of macro and microstructural state and the phase composition of Cu–30 vol. % $Fe_3C$ nanocomposites obtained by mechanical alloying of copper and iron powders in the liquid source of carbon (xylene) followed by thermal treatment were studied by means of X-ray phase analysis, Mössbauer spectroscopy, scanning electron and optical microscopy, measurement of dynamic magnetic susceptibility. It was demonstrated that iron carbides are not formed during alloying; however, for the alloys obtained by grinding for 96 h, annealing at a temperature above 500 °C leads to the formation of cementite with the volume fraction of about 30 %. The grain size of the copper matrix of this composite is 10 nm, while after annealing at 800 °C it is 30 nm.

**Key words:** mechanical alloying, nanocomposites, copper, cementite

## INTRODUCTION

It is impossible to produce bulk Cu–$Fe_3C$ composites using traditional metallurgic methods. Nanostructured copper alloys with the volume concentration of cementite 25?30 % is mechanical alloying (MA) of copper, iron and graphite powders followed by thermal treatment and compaction are produced most successfully [1–3]. Composites on the ground of copper and carbides of transition metals are promising as electrode materials because of high electric and thermal conductance, hardness, stability of electrophysical characteristics at increased temperatures, resistance to corrosion *etc*. [4–8]. Necessary parameters are provided by adding a relatively small amount of transition metal and graphite or carbide of transition metal (not more than 10 vol. %) [5, 6, 9]. However, the low content of strengthening phase brings complications into the technology of Cu–$Fe_3C$ alloy production. Copper is a very plastic material, and its treatment in a ball planetary mill with insufficient amount of graphite leads to its agglomeration and adhering to balls and the walls of mill containers. As a consequence, it is unreasonable to obtain powdered alloys of copper with the volume concentration of cementite up to 10 % using MA without adding special reagents preventing adherence. As a rule, to prevent agglomeration, some amount of alcohol, heptane, toluene or so is added into the mill containers [10]. We established experimentally that powder composites based on copper with cementite content 5–10 % may be obtained by MA only in liquid oxygen-free media. It is known [11–13] that cementite is easily formed during mechanical activation of iron in toluene, heptane *etc*. However, up to now the possibility of the production of Cu–$Fe_3C$ mechanocomposites using liquid hydrocarbons as carbon source and the effect of liquid grinding medium on MA in Cu–$Fe_3C$ system has not been studied yet.

The goal of the present work was to obtain Cu–$Fe_3C$ nanocomposites by MA of copper and iron powders in a liquid hydrocarbon (xylene),

to study their structural and phase state and to choose optimal synthesis regimes.

## EXPERIMENTAL

Model composites with the composition Cu–30 vol. % $Fe_3C$ were obtained by means of the high-energy mechanical activation of a mixture of copper and iron powders with the mass concentration of copper 72.7 % (99.72 mass %, average particle size 18 mm), iron 25.5 % (98 mass %, admixtures: nitrogen 0.6 mass %, oxygen 0.42 mass %, carbon 0.8 mass %, particle size 3–20 μm) in approximately 20 $cm^3$ of xylene $C_6H_4(CH_3)_2$ of ch. d. a. reagent grade. Mechanical activation was carried out in a Pulverisette-7 ball planetary mill (Fritsch) with energy strain of 2.0 W/g with forced air cooling. Heating of the external wall of containers during mill operation did not exceed 80 °C. Grinding tools were cylindrical containers (45 $cm^3$ in volume) and balls (20 sp., 10 mm in diameter) made of ShKh15 grade steel. For each assigned time of MA ($t_{MA}$ = 3, 6, 12, 24, 48, 96 h) the mass of charged powder mixture was 10 g. After MA, the powders were additionally thermally treated in argon atmosphere (with preliminary evacuation for forevacuum) at 600 and 800 °C for 1 h.

The analysis of the structural phase state of alloys was carried out on a DRON-3M X-ray diffractometer in monochromatic (graphite) copper radiation at room temperature. The qualitative and quantitative analyses of the recorded spectra was carried out with the help of software package developed at MISIS. The grain size of crystal copper was estimated from the diameter of coherent scattering regions determined by means of Warren–Acerbic procedure from the profile of one line (311) according to [14]. Mössbauer studies were carried out at room temperature using a YaGRS-4M spectrometer in the mode of constant accelerations with $^{57}Co$ γ-radiation source in the matrix of chromium and rhodium. The functions $P(H)$ of distribution of superfine magnetic fields (SFMF) were found using the generalized regular algorithm of inverse problem solution according to Tikhonov's procedure [15]. Thermomagnetic measurements were carried out using a set-up for the investigation of dynamic magnetic susceptibility (DMS) with the amplitude of alternate magnetic field 0.8 E and frequency 5 Hz in inert atmosphere (Ar) with the rate of 30 °C/min within temperature range 5–800 °C. The size of copper and iron particles was determined with the help of laser diffraction analyzer Analysette 22 Economy. Auger spectra and images in secondary electrons were obtained with a JAMP-10S spectrometer at the accelerating voltage of 10 kV, current $10^{-7}$ A, electron probe diameter 300 nm. Microstructure was studied using a MIM-8M optical microscope. Polished sections were etched with a 10 % solution of ferric chloride in ethanol.

## RESULTS AND DISCUSSION

Electron microscope images of powders obtained at $t_{MA}$ = 6, 48 and 96 h indicate that after grinding for 6 h the characteristic particle size is nearly 10 μm, after 48 h it does not exceed 5 mm (Fig. 1). The size distribution of particles is rather uniform. The analysis of the microstructure of particles obtained with $t_{MA}$ = 6 h (Fig. 2, *a*) showed that the particles are composed of copper with rounded inclusions of iron 0.5–10 μm in size, distributed uniformly inside copper particles. Iron is less plastic than copper, so during mechanical treatment iron particles get surrounded by copper layer. On the basis of size and shape of initial particles of iron powder, it may be concluded that the rate of iron inclusion grinding is insignificant at the initial stage of mechanical treatment ($t_{MA}$ = 6 h). This may be due to relatively small size of particles in initial iron powder which is 10 μm as average. It was shown in [16, 17] that this is the limiting value for the average particle size of iron powder ground in liquid organic medium.

After grinding for a longer time ($t_{MA}$ = 96 h), the morphology of copper powder becomes more disperse (see Figs. 1 and 2, *b*), while the size of copper particles in the powder is less than 1 μm. The formation of agglomerates of very small particles (see Fig. 1, *c*, *d*) is likely to be connected with the conditions of sample preparation to electron microscopic studies. According to the results of metallographic studies of the thin section of MA powder there

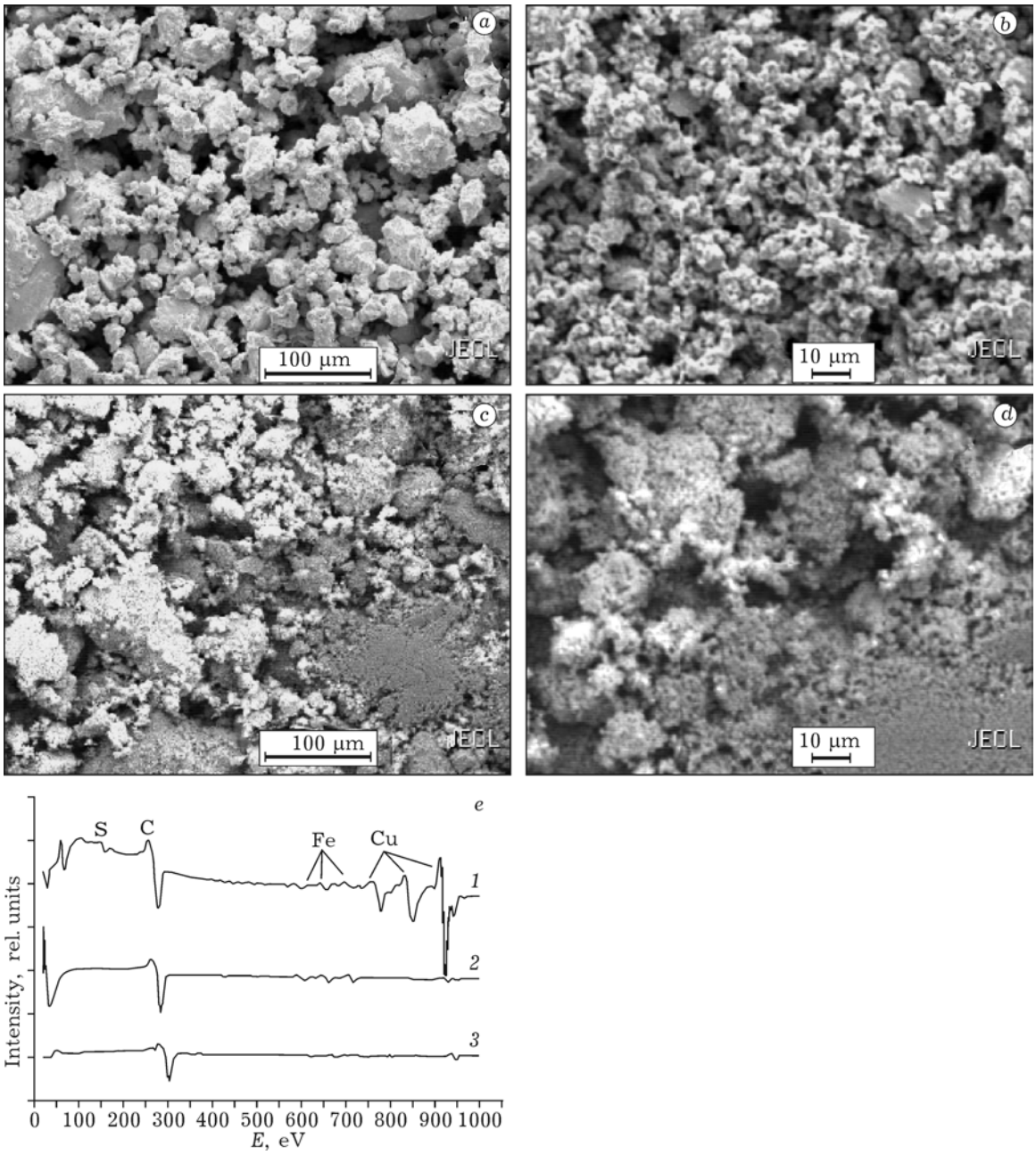


Fig. 1. Electron microscope images of powders subjected to mechanical alloying (MA) (*a*–*d*) and their Auger spectra (*e*). Time of MA, h: 6 (*a*), 48 (*b*), 96 (*c*, *d*): *1*–*3* – Auger spectra of powders with MA time 6, 49 and 96 h, respectively.

are not agglomerates; light particles of MA alloy are uniformly distributed over the dark binding matrix of epoxide glue (see Fig. 2, *b*).

Carbon concentration on the surface of particles increases up to 92 at. % with an increase in grinding time (the rest 8 at. % are copper and iron), which follows from the results of Auger analysis (see Fig. 1, *e*) and is the evidence of intense xylene decomposition process. Xylene destruction occurs mainly on the surface of grinding balls and container because iron serves as a catalyst for the decomposition of liquid hydrocarbons [13].

According to the data of X-ray structural analysis of powders (Fig. 3), the phase composition of the samples after MA is represented by crystalline Cu and Fe. It follows from the calculations of the size of coherent scattering

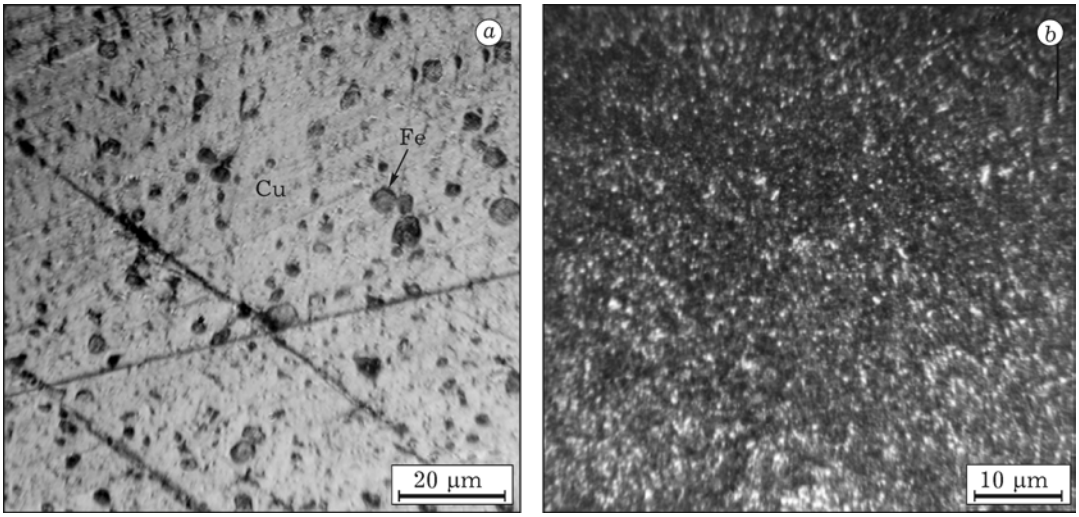


Fig. 2. Microstructure of powders after MA for 6 (*a*) and 96 h (*b*).

regions that both phases are nanocrystalline even after powder grinding for 6 h. Within the determination error, the lattice parameter of iron is close to the reference value and does not depend on the time of mechanical treatment. The lattice parameter of copper (0.3615 nm) increases with grinding time and reaches 0.3639 nm for 96 h (Fig. 4) as a consequence of the formation of the solid solution of iron substitution in FCC copper [18–20].

The formation of the solid solution of Cu–Fe substitution is confirmed by the appearance of D1 doublet of the paramagnetic phase in Мцssbauer spectra of MA powders with the isomeric shift parameters IS = 0.13(1) mm/s, quadrupole splitting QS = 0.50(1) mm/s (Fig. 5, plot *1*) which correspond, according to [21], to iron atoms in copper lattice with two or more neighbouring iron atoms. At the same time, paramagnetic nanoclusters of BCC iron in copper matrix may have close parameters of the doublet [22, 23]. It is necessary to stress that the spectrum of powder with $t_{MA}$ = 12 h exhibits two doublets of paramagnetic phases. The values of IS = 0.30(2) mm/s and QS = 1.02(4) mm/s of D2 doublet, which has a smaller area, are close

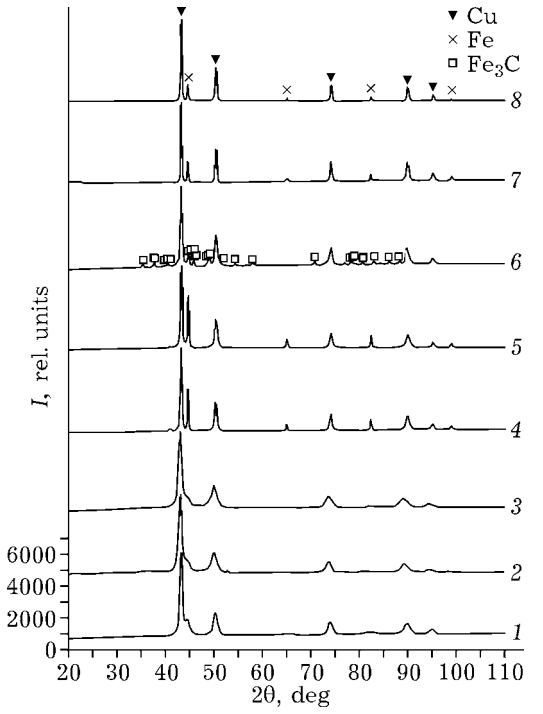


Fig. 3. Diffraction pattern of powders subjected to mechanical alloying for 6, 48, 96 h (*1–3*, respectively), then annealed at 600 °C (*4–6*, respectively) and 800 °C (*7*, *8*, respectively).

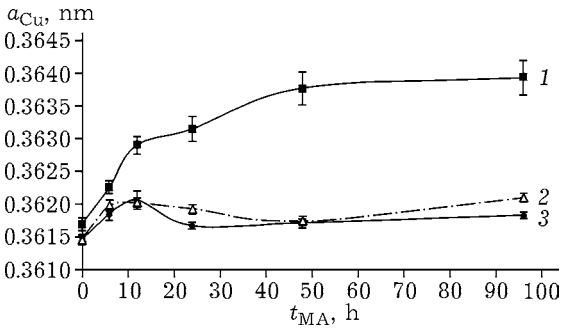


Fig. 4. Dependences of copper lattice parameter (*a*) on powder MA time before (*1*) and after annealing at 600 (*2*) and 800 °C (*3*).

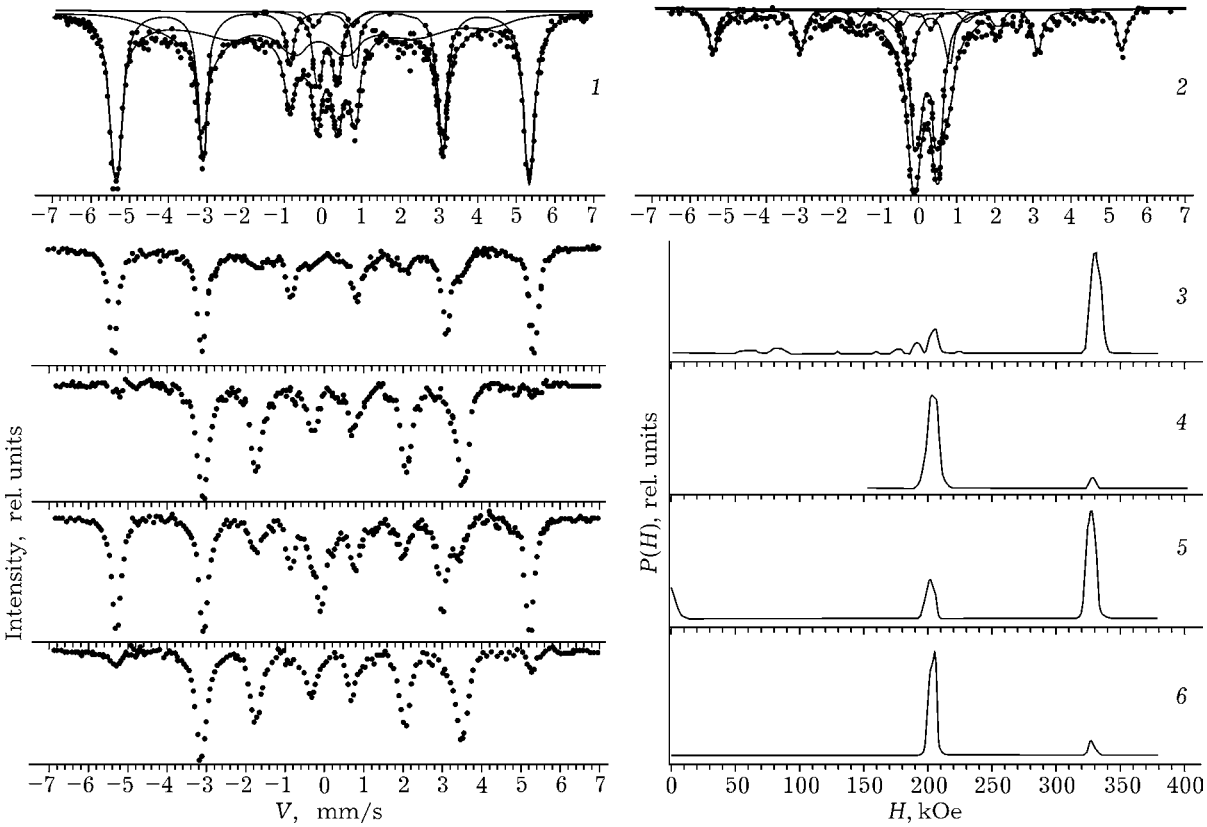


Fig. 5. Mössbauer spectra and corresponding distribution functions $P(H)$ for powders subjected to mechanical alloying for 12 and 96 h (*1*, *2*, respectively) and annealed at 600 °C (*3* and *4*, respectively) and 800 °C (*5* and *6*, respectively).

to the corresponding parameters for phases based on copper oxide $Cu_2O$ in which some copper atoms are substituted by iron atoms [24–26].

With an increase in grinding time to 96 h, the area of the doublets and the corresponding fraction of paramagnetic phases increase (see Fig. 5, plot *2*). The parameters of D2 doublet are conserved, while those of D1 somewhat increase up to IS = 0.22(1) mm/s and QS = 0.56(1) mm/s. Iron content in the oxide phase increases from 0.5 to 4 at. %, and from 2 to 11 at. % in the solid substitution solution of iron in copper, which accounts for almost half of total iron in the alloy. The spectrum of the sample with $t_{MA}$ = 96 h contains iron carbide phases, accounting for almost 5 at. %. It does not appear possible to determine the type and composition of carbide phases.

So, with an increase in $t_{MA}$, the degree of iron dissolution in copper and the fraction of solid solution increase; no noticeable formation of iron carbides occurs. Carbon is likely to be accumulated on the surface of copper particles, in interfacial regions and along grain boundaries, but does not penetrate inside grains. For the formation of iron carbides, it is necessary to increase the diffusion mobility of carbon and perhaps iron, which is realized during the thermal treatment of the resulting composites.

The appearance of temperature dependences of DMS (Fig. 6) depicts the occurrence of magnetic and phase transitions in the obtained composites. A small region of DMS drop at a temperature of about 200 °C for the alloy with $t_{MA}$ = 96 h corresponds to the transition into the paramagnetic state of cementite formed during MA.

Within temperature range of 250–450 °C, the decomposition of the paramagnetic FCC solid solution of iron in copper [27–30] and an increase in DMS occur as a consequence of the formation of clusters of ferromagnetic BCC iron. A drop at 320–330 °C is close to Curie temperature for supersaturated solid solution of copper in α-Fe with the atomic concentration of copper 3 % and higher [31]. The presence of the solid solution of copper in iron is addi-

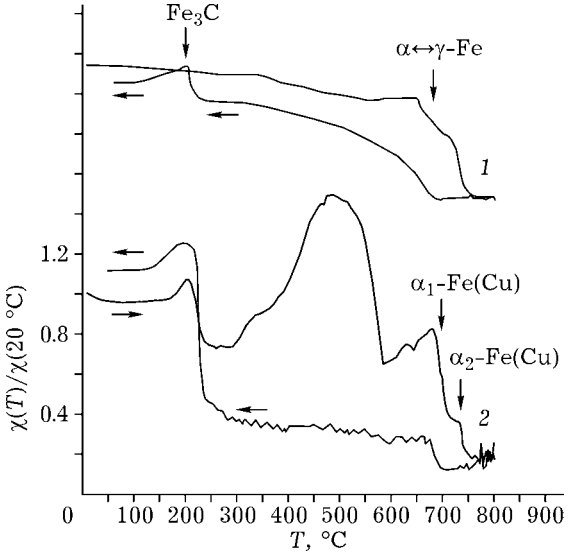


Fig. 6. Temperature dependences of the dynamic magnetic susceptibility (heating and cooling) $\chi(T)$ for powders subjected to MA for 12 (*1*) and 96 h (*2*).

tionally confirmed also by magnetic transformations in $\alpha_1$-Fe(Cu) and $\alpha_2$-Fe(Cu) phases with copper content 0.5–0.6 ($\alpha_1$) and 0.2–0.3 at. % of Cu ($\alpha_2$), respectively [31, 32]. This is manifested as declines on DMS curves at temperatures 650–680 and 720–730 °C, respectively. It is evident that along with the supersaturated solid solution of iron in copper, MA also leads to the formation supersaturated solution of copper in iron, and both phases decompose almost completely during heating. It is difficult to determine the composition of the solid solution of copper in iron in MA samples by means of X-ray diffraction and Mössbauer spectroscopy because of relatively small fraction of nanostructural iron.

At $T > 500$ °C, the magnetic susceptibility of alloys decreases substantially as a consequence of thermally induced formation of cementite. Evidently, at this temperature carbon starts to interact both with nanocrystalline iron that did not dissolve in the copper matrix of the alloy during MA and with iron clusters evolved as a result of decomposition of supersaturated solid solutions. The larger is the amount of solid solution formed during MA and the smaller is the size of iron particles that did not dissolve in copper matrics, the larger amount of cementite is formed.

Results of investigations by means of X-ray structural analysis and Mössbauer spectroscopy of alloys annealed at a temperature of 600 and 800 °C confirm the above-formulated conclusions. A decrease of the lattice parameter of copper to 0.3620(2) nm after annealing at 600 °C and to 0.3617(1) nm at 800 °C (see Fig. 4)

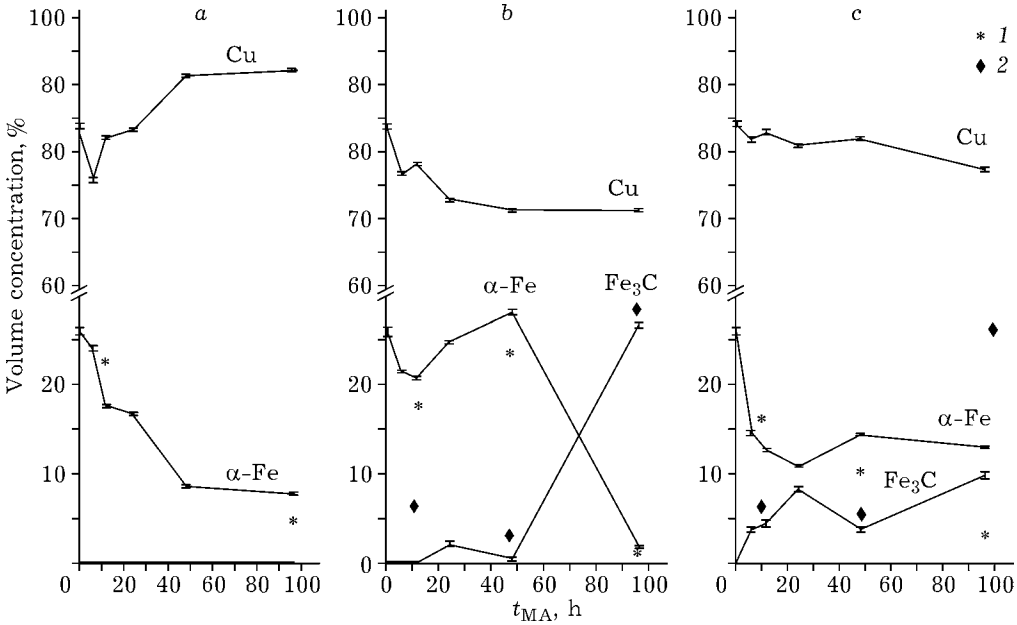


Fig. 7. Volume concentrations of phases Cu, α-Fe and $Fe_3C$ for MA powders before (*a*) and after annealing at 600 (*b*) and at 800 °C (*c*) determined by means of XSA: *1* – α-Fe, *2* – $Fe_3C$, determined by means of Mössbauer spectroscopy.

is due to the decomposition of supersaturated solid solution of iron in copper and the conservation of 2–3 at. % of iron in copper [33]. The fraction of cementite in the phase composition of alloys obtained after $t_{MA} < 96$ h does not exceed 7 vol. %, which follows from the data shown in Fig. 7. For the maximal grinding time (96 h) and independently of annealing temperature, the volume concentration of cementite is nearly 30 %. Evaluation by means of Mössbauer spectroscopy gives larger volume concentrations of phases because the copper matrix of the alloys is nanocrystalline, while the formed cementite is characterized by high dispersity degree.

The grain size in dispersion-strengthened alloys is one of the most essential factors determining their hardness. The size of coherent areas for the copper matrix of alloys (Fig. 8) after MA do not exceed 10 nm, after annealing at 600 °C – 12 nm. Annealing at 800 °C leads to some increase in the grain size – up to 60 nm; with an increase in the grinding time a trend is observed to decrease the grain size to 30 nm as a result of thermal treatment. The fact that the nanocrystalline structure of copper matrix in alloys is conserved at a temperature much higher than copper recrystallization temperature (about 300 °C) for MA time shorter than 96 h is due to the presence of excess carbon on the boundaries of copper and iron nanograins. Carbon forms clusters on grain boundaries, as shown in [34, 35] for MA composites Cu–C as example, and slows down diffusion at grain boundaries thus limiting the growth of copper nanograins. For powder grinding time longer than 96 h, the maximal possible cementite fraction formed during thermal treatment is provided due to the minimal sizes of particles and grains of copper and iron, large specific surface of the powder and high concentration of carbon on the surface of particles and nanograins boundaries. In this case, the size of grains of the matrix of annealed alloy decreases because of thermally activated nucleation of a large number of disperse inclusions of cementite at the boundaries of copper nanograins.

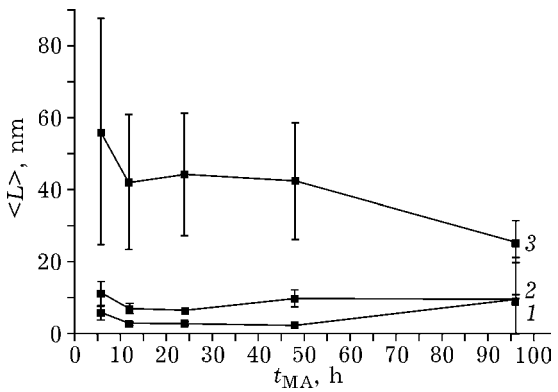


Fig. 8. Dependence of the coherence area size of copper on MA time for powders before (*1*) and after annealing at 600 (*2*) and 800 °C (*3*).

## CONCLUSION

Features of cementite formation in copper matrix during mechanical alloying followed by thermal treatment of Cu–Fe powders in the liquid organic medium (xylene) were studied in the work.

It is shown that with xylene as the grinding medium and carbon source, supersaturated solid solutions of iron in FCC copper and copper in bcc iron are formed after the transition of initial components of the alloy into nanostructured state. Iron carbides are not formed, independently of the duration of mechanical alloying. Long-term mechanical treatment (96 h) followed by annealing of the resulting alloys at a temperature above 500 °C lead to the formation of 30 vol. % cementite in the nanocrystalline copper matrix with grain size below 30 nm. The nanocrystalline state of the copper matrix of the formed composites is conserved after annealing at 800 °C.

## Acknowledgements

The authors thank L. E. Bodrova for the provided copper powders, D. V. Surnin for conducting electron microscopic studies and D. S. Rybin for the analysis of particles of powders.

## REFERENCES

1 Caravaiho P. A., Fonesca L., Marques M. T., Correia J. B., Almeida A., Viar R., *Acta Mater.*, 53 (2005) 967. URL: http://www.sciencedirect.com/scence/article/pii/S1359645404006652

2 Correia J. B., Marques M. T., *Mater. Sci. Forum,* 455–456 (2004) 501.

3 Correia J. B., Marques M. T., Caravaiho P. A., Vilar R. *J. Alloys Compounds,* 434–438 (2007) 301.

4 Raikov Yu. N., Ashikhmin G. V., Nikolaev A. K. Revina N. I., Kostin S. A., *Metallurg,* 8 (2007) 40.

5 Ichikawa K. and Achikita M., *Mater. Trans. JIM,* 34, 8 (1993) 718.
6 Long B. D., Umemoto M., Todaka Y., Othman R., Zuhailawati H., *Mater. Sci. Eng. A.,* 528 (2011) 1750.
7 Palma R. H., Sepъlveda A. H., Espinoza R. A., Montiglio R. C., *Mater. Proc. Technol.,* 169, 1 (2005) 62.
8 Long B. D., Othman R., Umemoto M., Zuhailawati H., *J. Alloys Compounds,* 505 (2010) 510.
9 López M., Camurri C., Vergara V., Jiménez J. A., *Rev. Metal. Madrid,* 41 (2005) 308.
10 Khodakov G. S., Fizika Izmelcheniya, Nauka, Moscow, 1972.
11 Inventor's Certification No. 1678525 Al SU, 1991.
12 Yelsukov E. P., Barinov V. A., Ovetchkin L. V., *J. Mater. Sci. Lett.,* 11 (1992) 662.
13 Lomaeva S. F., *FMM,* 104, 4 (2007) 403.
14 Dorofeev G. A., Streletskiy A. N., Povstugar I. V., Protasov A. V., Elsukov E. P., *Kolloid. Zh.*, 74, 6 (2012) 710.
15 Voronina E. V., Ershov N. V., Ageev A. L., Babanov Yu. A., *Phys. Star. Sol. (B),* 160 (1990) 625.
16 Elsukov E. P., Lomaeva S. F., Konygin G. N., Dorofeev G. A., Povstugar V. I., Mikhaylova S. S., Zagaynov A. V., Maratkanova A. N., *FMM,* 87, 2 (1999) 33.
17 Vasiliev L. S., Lomaeva S. F., *FMM,* 93, 2 (2002) 66.
18 Crivello J.-C., Nobuki T. and Kuji T., *Mater. Trans.,* 49, 3 (2008) 527.
19 Lucas F. M., Trindade B., Costa B. F. O., Le Caër G., *Key Eng. Mater.,* 230–232 (2002) 631.
20 Harris V. G., Kemner K. M., Das B. N., Koon N. C. and Ehrlich A. E., *Phys. Rev. B.,* 54, 10 (1996) 6929.
21 Dunlap R. A., Eelman D. A., Mackay G. R., *J. Mater. Sci. Lett.*, 17 (1998) 437.
22 Suzdalev I. P., Maksimov V. V., Imshennik V. K., Novichikhin S. V., Matveev V. V., Gulilin E. A., Chekanova A. E., Petrova O. S., Tretyakov Yu. D., *Ros. Nanotekhnol.,* 2, 5?6 (2007) 73.
23 Campbell S. J., Clark P. E. and Liddell P. R., *J. Phys. F.: Metal. Phys.,* 2 (1972) L114.
24 Ogale S. B., Bilurkar P. G., Joshi S., Marest G., *Phys. Rev. B.,* 50, 14 (1994) 9743.
25 Stewart S. J., Goya G. F., Punte G. and Mercader R. C., *J. Phys. Chem. Sol.,* 58, 1 (1997) 73.
26 Joseph D. P., David T. P., Raja S. P., Venkateswaran C., *Mater. Charact.,* 59 (2008) 1137.
27 Jiang J. Z., Pankhurst Q. A., Johnson C. E., Gente C. and Bormann R., *J. Phys.: Condens. Matter,* 6 (1994) L227.
28 Eckert J., Holzer J. C. and Johnson W. L., *J. Appl. Phys.,* 73, 1 (1993) 131.
29 Macri P. P., Enzo S., Cowlam N., Frattini R., Principi G. and Hu W. X., *Phil. Mag. B.,* 71, 2 (1995) 249.
30 Eilon M., Ding J. and Street R., *J. Phys.: Condens. Matter,* 7 (1995) 4921.
31 Keune W., Lauer J. and Williamson D. L., *J. de Physique,* 35, 12 (1974) C6-473.
32 Pearson W. B., Handbook of Lattice Spacings and Structures of Metals and Alloys, Pergamon Press, London *etc.*, 1958.
33 Uenishi K., Kobayashi K. F., Nasu S., Hatano H., Ishihara K. N. and Shingu P. H., *Z. Metallkd.,* 83 (1992) 132.
34 Marques M. T., Correia J. B., Conde O., *Scripta Mater.*, 50 (2004) 963.
35 Jin Y. and Hu M., *Adv. Mater. Res.*, 306–307 (2011) 1747.